JACS Au
AN OPEN ACCESS JOURNAL OF THE AMERICAN CHEMICAL SOCIETY

pubs.acs.org/jacsau
Article

Harnessing Dpp-Imine as a Powerful Achiral Cocatalyst to Dramatically Increase the Efficiency and Stereoselectivity in a Magnesium-Mediated Oxa-Michael Reaction

Yingfan Xu,[§] Dan Liu,[§] Feiyun Gao, Shixin Li, Xiaoyong Zhang,* Linqing Wang,* and Dongxu Yang*

Cite This: *JACS Au* 2024, 4, 164−176
Read Online

ACCESS | Metrics & More | Article Recommendations | Supporting Information

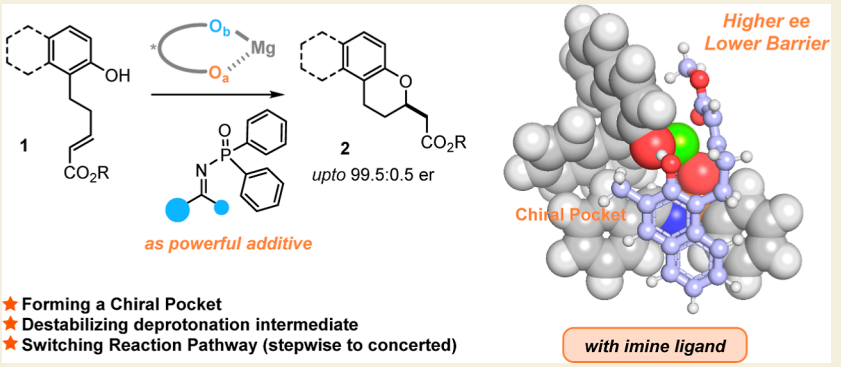

ABSTRACT: Dpp-imines are classic model substrates for synthetic method studies. Here, we disclose their powerful use as achiral coligands in metal-catalyzed reactions. It is highly interesting to find that the Dpp-imine can not only act as powerful ligand to create excellent chiral pockets with magnesium complexes but also, more importantly, this coligand can dramatically enhance the catalytic ability of the metal catalyst. The underlying reaction mechanism was extensively explored by conducting a series of experiments, including ^{31}P NMR studies of the coordination complex between the Dpp-imine coligand and magnesium complexes, ESI capture results, multiple control experiments, studies and comparison of different coligands, ^{1}H NMR studies on the relationship between the substrate and Dpp-imine coligand, as well as the relationship between the substrate and the full complexes. Furthermore, DFT calculation provided valuable insights in the role of the imine additive and demonstrated that adding the Dpp-imine coligand in the magnesium catalyst can switch the deprotonation/nucleophilic addition steps from a stepwise mechanism to a concerted process during the oxa−cyclization reaction. The crucial factors responsible for the excellent enantioselectivity and enhanced reaction efficiency brought by Dpp-imine have been extracted from the calculation model. These mechanistic experiments and DFT calculation data clearly disclose and prove the powerful and interesting functions of the Dpp-imine coligand, which also direct a novel application of this type of active imine as useful ligands in metal-catalyzed asymmetric reactions.

KEYWORDS: *magnesium catalysis, achiral coligand, enhanced catalytic efficiency, stereoselectivity, oxa-Michael reaction, mechanism studies*

INTRODUCTION

Imines are important and basic synthetic feedstocks in chemical synthesis and are widely utilized as model substrates in many classic reactions, including under catalytic asymmetric patterns (Scheme 1, A).[1−12] On the other hand, the nonactive imine, usually called Schiff base, represents one of the mainstream ligands that are employed in a series of metal-catalyzed transformations. It is well-known that the usual Schiff base ligands possessing multiple coordination sites are always generated from primary aromatic or aliphatic amines.[13−23] However, attempts of applying active and easily accessed imines, including Boc-, Ts-, or Dpp-imine, as ligands in metal catalysis is still elusive, given that these imines are often utilized as model substrates in asymmetric reactions.[24−39] There exist several potential challenges for utilizing these active monoimines as ligands in metal catalysis: (a) active monoimines might not be as enough as ligands; (b) these active imines are typically electrophiles which are prone to react with a wide scope of given nucleophiles; (c) in the situation of asymmetric reactions, it might be hard to introduce valid chiral elements in the classic

Received: October 2, 2023
Revised: December 6, 2023
Accepted: December 11, 2023
Published: December 21, 2023

https://doi.org/10.1021/jacsau.3c00584
JACS Au 2024, 4, 164−176

Scheme 1. Concept of Harnessing Imine as a Powerful Cocatalyst in Asymmetric Reaction

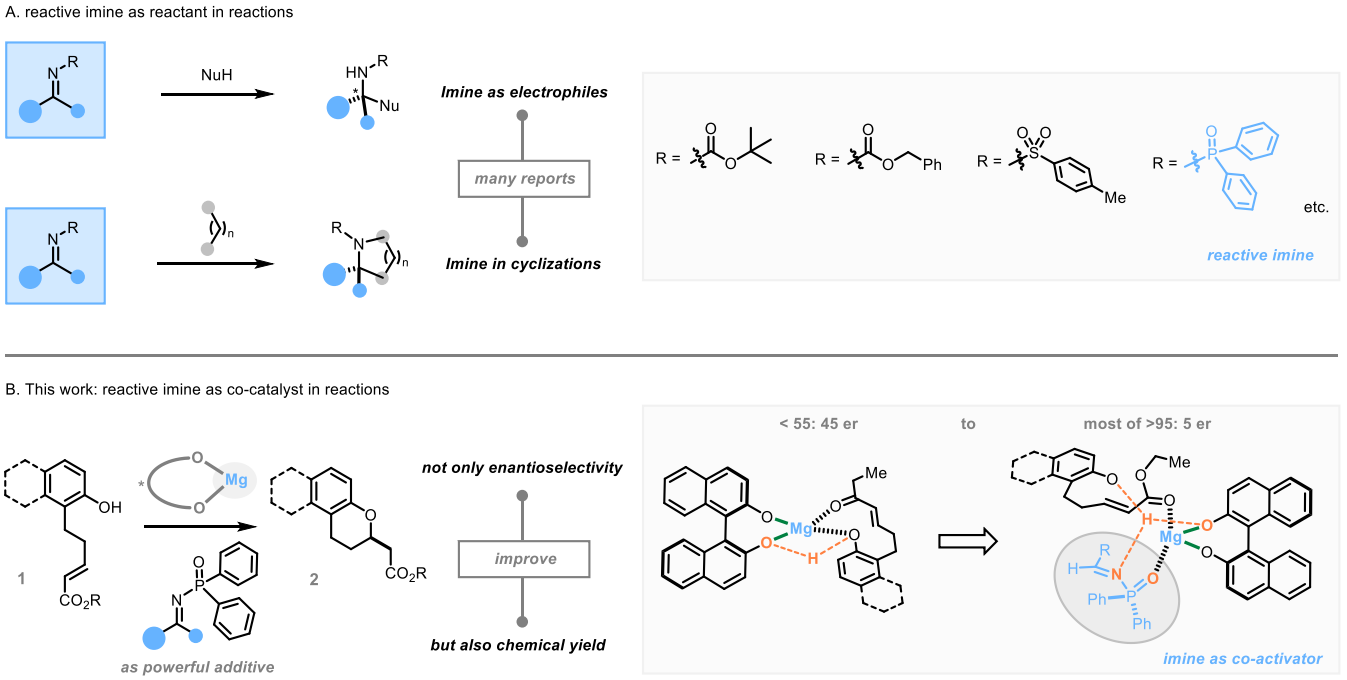

Scheme 2. Optimization of the Oxa−Cyclization Reaction by the Introduction of the Imine Coactivator Strategy

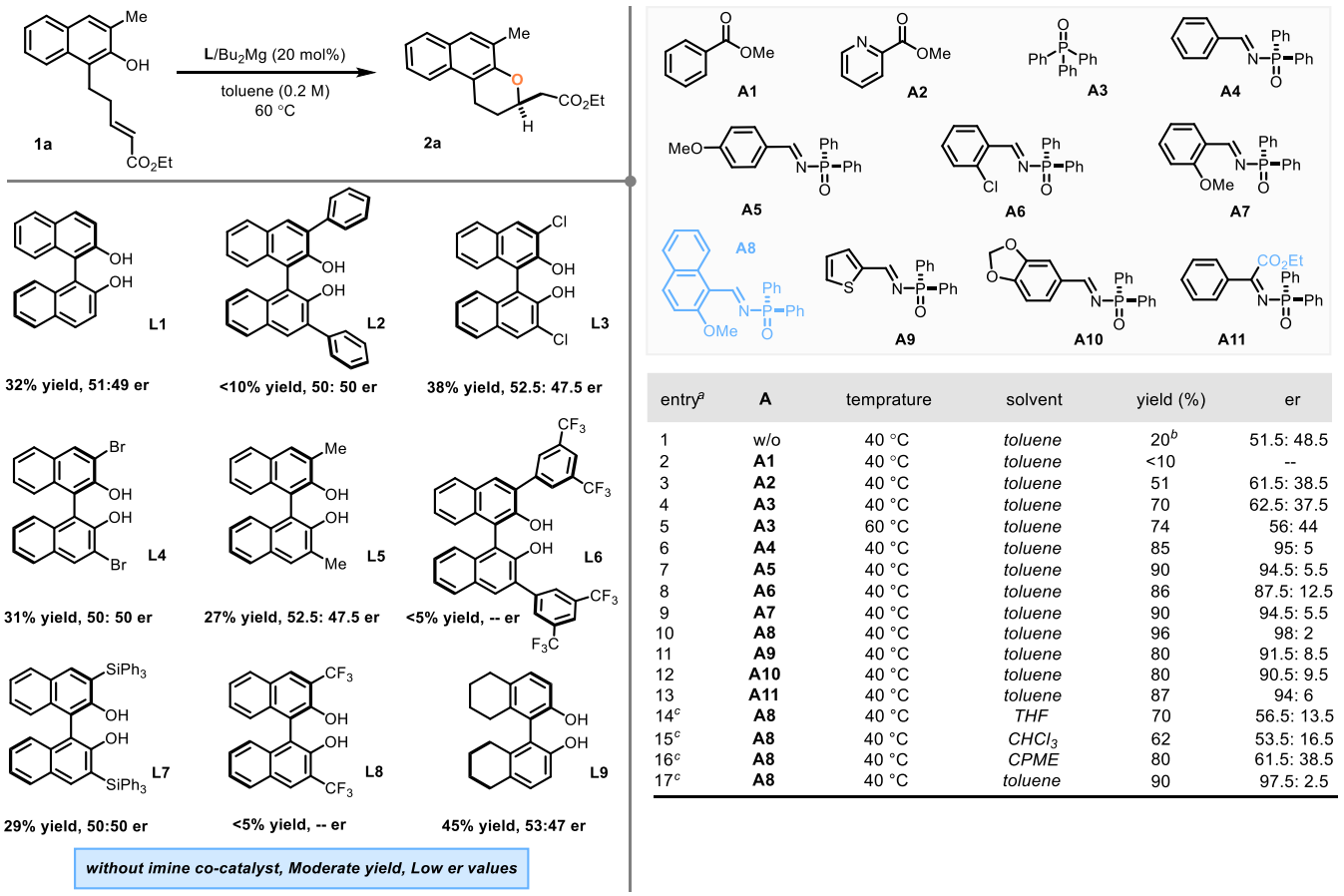

entry[a]	A	temprature	solvent	yield (%)	er
1	w/o	40 °C	*toluene*	20[b]	51.5: 48.5
2	**A1**	40 °C	*toluene*	<10	--
3	**A2**	40 °C	*toluene*	51	61.5: 38.5
4	**A3**	40 °C	*toluene*	70	62.5: 37.5
5	**A3**	60 °C	*toluene*	74	56: 44
6	**A4**	40 °C	*toluene*	85	95: 5
7	**A5**	40 °C	*toluene*	90	94.5: 5.5
8	**A6**	40 °C	*toluene*	86	87.5: 12.5
9	**A7**	40 °C	*toluene*	90	94.5: 5.5
10	**A8**	40 °C	*toluene*	96	98: 2
11	**A9**	40 °C	*toluene*	80	91.5: 8.5
12	**A10**	40 °C	*toluene*	80	90.5: 9.5
13	**A11**	40 °C	*toluene*	87	94: 6
14[c]	**A8**	40 °C	*THF*	70	56.5: 13.5
15[c]	**A8**	40 °C	$CHCl_3$	62	53.5: 16.5
16[c]	**A8**	40 °C	*CPME*	80	61.5: 38.5
17[c]	**A8**	40 °C	*toluene*	90	97.5: 2.5

structure of active monoimines; and (d) the inflexible impression of these types of imines as "classic model substrates". On consideration of these above reasons, we wondered whether it is possible to explore these active imines as ligands or coligands in metal-catalyzed reactions, which might benefit the discovery of new types of active imine ligands in organic synthesis. Moreover, the utilization of active monoimines as coligands

https://doi.org/10.1021/jacsau.3c00584
JACS Au 2024, 4, 164−176

Scheme 3. Substrate Scope of the Oxa−Cyclization Reaction under the Imine Coactivator Strategy

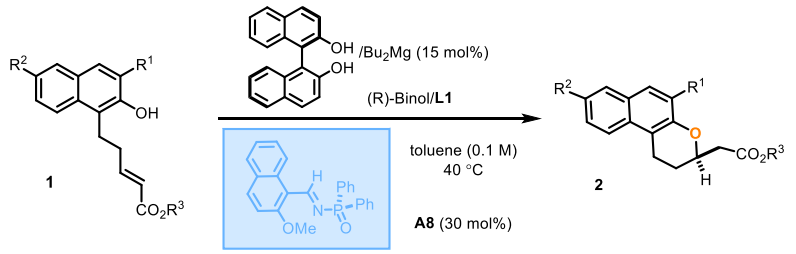

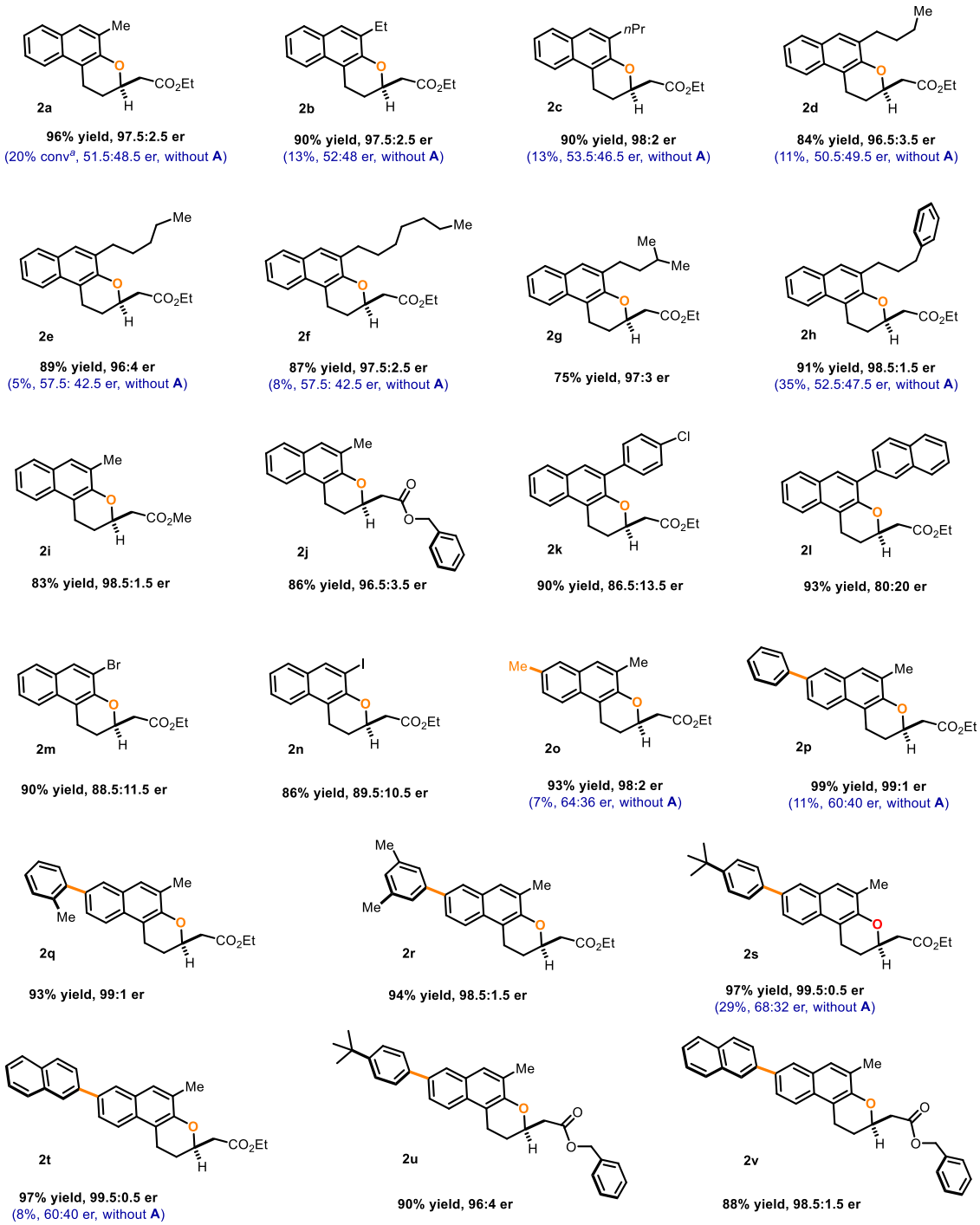

might be a feasible and alternative strategy in metal-catalyzed asymmetric reactions.

On the basis of our continuous works on in situ-generated magnesium catalysts[40−53] and especially the recent finding that Dpp-imines are prone to coordinate to the Mg(II) center,[54] we

https://doi.org/10.1021/jacsau.3c00584
JACS Au 2024, 4, 164−176

here attempted to use Dpp-imine as a pivotal coligand with the in situ-generated magnesium catalysts and to clarify their multiple and interesting functions in catalytic asymmetric reactions. Based on these intense works on and the importance of asymmetric construction of chiral α-substituted cyclic ethers including chroman or benzo[c]chroman skeletons,[55−62] we selected oxa-Michael reaction[63−72] as the typical conjugate reaction[73−80] model to test this idea with the aim to study the functions of the active imine ligand in Mg(II) catalysis. Interestingly, in the current work, we found that this type of active monoimine coligand can not only dramatically improve the enantioselectivity but also obviously influence the activation mode and dramatically enhance the reactivity in the Mg(II)-mediated oxa-Michael reaction (Scheme 1, B).

RESULTS AND DISCUSSION

The selected oxa-Michael reaction was initially optimized by using naphthol **1a** as the substrate and using the in situ-generated magnesium catalyst from the commercially available Binol-type ligands (Scheme 2). A series of binaphthols derived from (R)-Binol were screened under mild conditions. It was found that the Mg(II) catalysts with less steric hindrance can promote the cyclization reaction with a moderate yield. However, disappointingly, all ligands screened in the current transformation led to almost racemic cyclization adducts **2a**.

Next, we screened achiral coligands in the Mg(II)-catalyzed oxa-Michael reaction at 40 °C (Scheme 2). Although adding a simple benzoate **A1** decreases the yield, the introduction of pyridine-2-carboxylate could enhance the efficiency of the cyclization process. We pleasingly observed a considerable increase of the ee value by using **A2**. Meanwhile, we found that triphenylphosphine oxide **A3** also elevated the reaction's yield and enantioselectivity (entry 3). Then, it becomes interesting to examine whether a ligand containing both a phosphonoxy group and a C═N bond could further improve the reaction efficiency and enantioselectivity. A series of Dpp-imines were screened, and fortunately we found that the readily available imine **A4**, derived from benzaldehyde, can effectively increase the efficiency and enantioselectivity, with the improvement of the er value to 95:5 (entry 4). With this exciting result in hand, we further synthesized and tried extensive Dpp-imines in the model reaction and eventually determined imine **A8** as the optimal achiral coligand. Notably, the imine derived from the ketone ester also gave a high level of enantioselectivity (entry 13).

Under the optimized conditions, we next extended the substrate scope of this intramolecular Michael reaction mediated by the Dpp-imine-assisted magnesium catalyst (Scheme 3). In the presence of the imine coligand, the naphthols with a wide tolerance of alkyl groups at the C3-position on the aromatic ring led to high level of enantioselectivities and good chemical yields. However, equipment of aryl groups at the C3-position gave relatively lower enantioselectivities (Scheme 3, **2k** and **2l**), and similarly, the introduction of halogens led to acceptable results. Different esters such as the benzyl group were also tolerable under the optimized conditions (Scheme 3, **2i** and **2j**). Moreover, the phenol substrates with aryl substitutions at C-6 positions also gave excellent results. Notably, we also examined the performance of several representative substrates in the Mg(II)-mediated cyclization reaction without the use of the imine coligand. The absence of an imine leads to the decrease of both chemical yield and er values. These above results clearly revealed that the Dpp-imine coligand not only performed as a powerful achiral additive to elevate the enantioselectivity but also acted as a cocatalyst to enhance the transformation efficiency.

Reactions with the representative phenol substrates were also evaluated, which showed moderate yields and higher er values. To determine the absolute configuration of the cyclization adduct, we synthesized compound **4** from the cyclization of substrate **1a** to give **2a** at a 2.0 mmol scale production, followed by the reduction of the ester group and functional group protection (Scheme 4).

Scheme 4. Further Extension of the Oxa−Cyclization Reaction and Confirmation of the Absolute Configuration

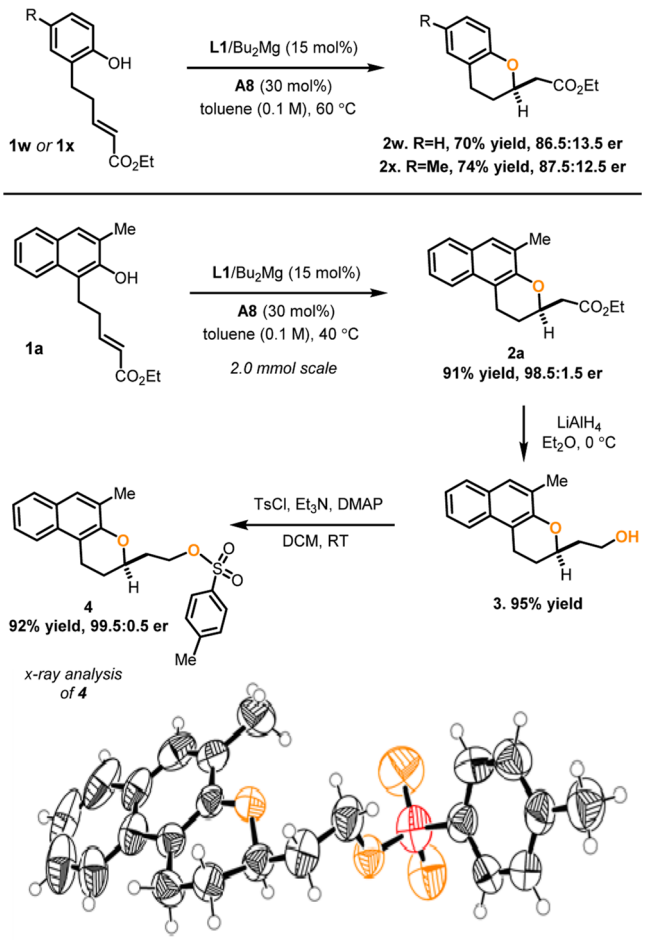

To illustrate how the DPP-imine coligand enhances the reaction's transformative efficiency and enantioselectivity, we performed a series of controlled and mechanistic experiments. Nonlinear effect studies disclosed a linear relationship between the ee values of ligand **L1** and oxa-Michael cyclization adduct **2a** (Figure 1A). This linearity result implies that in the presence of coligand **A8**, the active catalyst might be the monomer complex. The ESI analysis experiment also supports the single-metal center observation by the characterization of coordination complexes **I** (**L1**/**Mg**/**A8** = 1:1:1) and **II** (**L1**/**Mg**/**A8** = 1:1:2) (Figure 1F,G). Notably, under the mass spectrometry test conditions, imine **A8** could form complexes with the sodium cation accordingly, thus reducing the relative abundance of magnesium complexes (Figure 1E).

Further, ^{31}P NMR studies gave more evidence of the formation of complexes **I** and **II** (Figure 1D). Additionally, we also compared the transformations with a different coligand's

https://doi.org/10.1021/jacsau.3c00584
JACS Au 2024, 4, 164−176

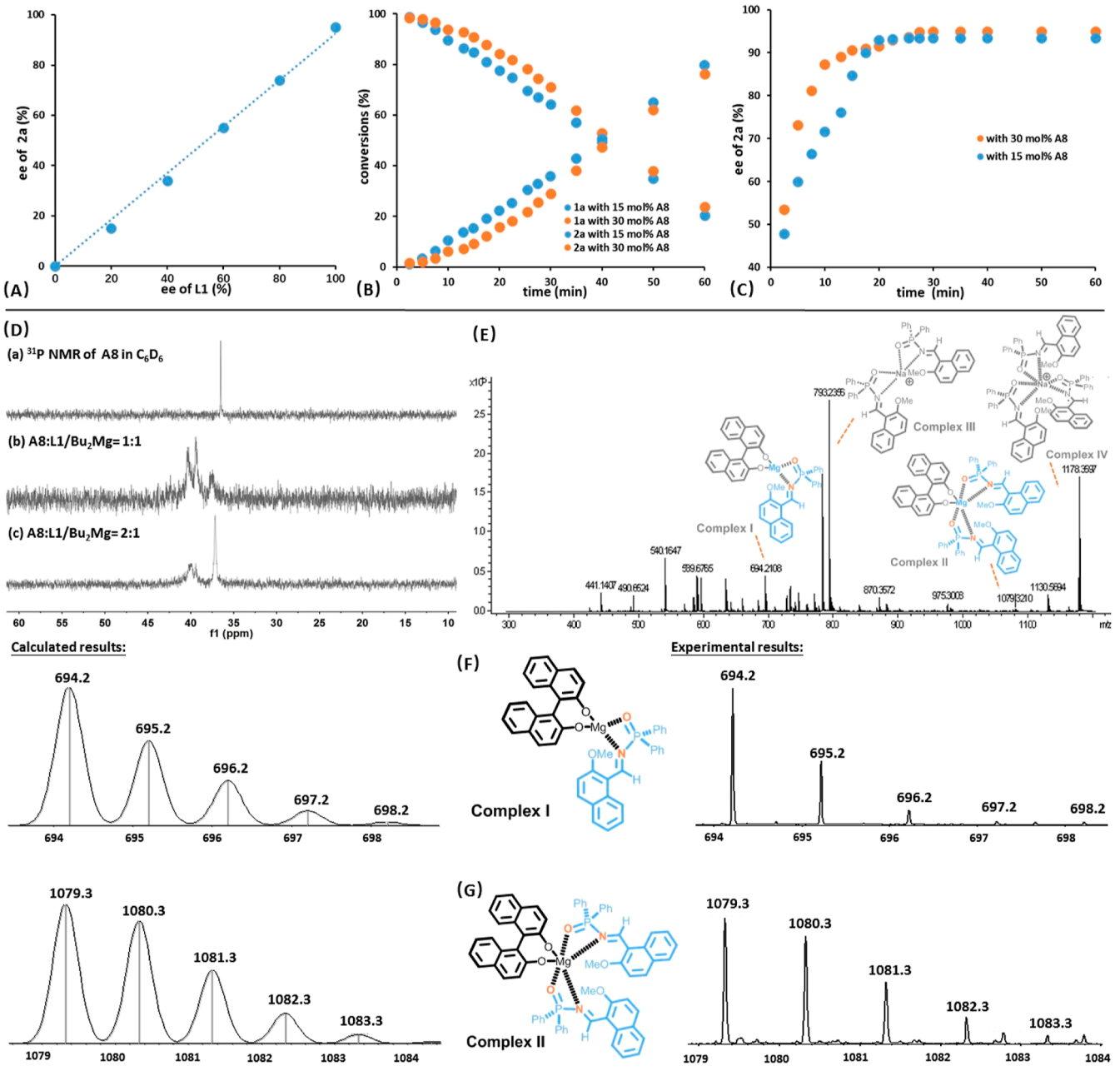

Figure 1. Investigation of the coordination details of the imine cocatalyst in the oxa−cyclization reaction. (A) Nonlinear effect studies of the reaction. (B) Reaction profile under different loading amounts of **A8**. (C) Enantioselectivities change during the reaction time with 15 and 30 mol % **A8** under 15 mol % **L1**/Bu_2Mg. (D) ^{31}P NMR studies of the relationship between the magnesium catalyst and **A8**. (E) HRMS analysis of the mixture of **L1**/Bu_2Mg and **A8** [the complexes were generated from **L1** (0.05 mmol), Bu_2Mg (50 μL, 1.0 M in heptane, 0.05 mmol), and **A8** (0.02 mmol)]. (F) Comparison of the calculated and experimental results of complex **I**. (G) Comparison of the calculation and experimental results of complex **II**.

(**A8**) loading amount (**L1**/**Mg**/**A8** = 1:1:1 vs **L1**/**Mg**/**A8** = 1:1:2). An interesting finding is that the conversion under 15 mol % **A8** is slightly faster than the situation of 30 mol % loading amount (Figure 1B). Besides, with the catalyst system of **L1**/**Mg**/**A8** = 1:1:2, the cyclization adduct **2a** could achieve a relatively high level of enantioselectivities in a shorter time (Figure 1C). We speculated that these results might be due to the formation of more than one complex with different coordination directions, as observed in the ^{31}P NMR analysis (Figure 1D). However, by adding 2.0 equiv of imine **A8** to **L1**/**Mg**, the favorable complex **I** leading to high er values formed more quickly through the coordination substitution of substrate **1a** with imine **A8**.

In the following experiments, we focused on the detailed functions of the coligand Dpp-imine **A8**. Screening of achiral coligands have pointed out that most coordination additives, including various imines, pyridine, and triphenylphosphine oxide (TPO), would greatly enhance the efficiency of the cyclization process (Figure 2A). Meanwhile, some of selected coligands obviously improved the enantioselectivities, implying that the coordination complexes forming from the coligands to **L1**/**Mg** can result in a more favorable chiral environment (Figure 2B). Among these selected coligands, Dpp-imine **A8** presents the most powerful chiral control conditions. On the other hand, we also carried out ^{1}H NMR analysis of the interactions between the phenol **1a** and **A8**, as well as the ^{1}H

https://doi.org/10.1021/jacsau.3c00584
JACS Au 2024, 4, 164−176

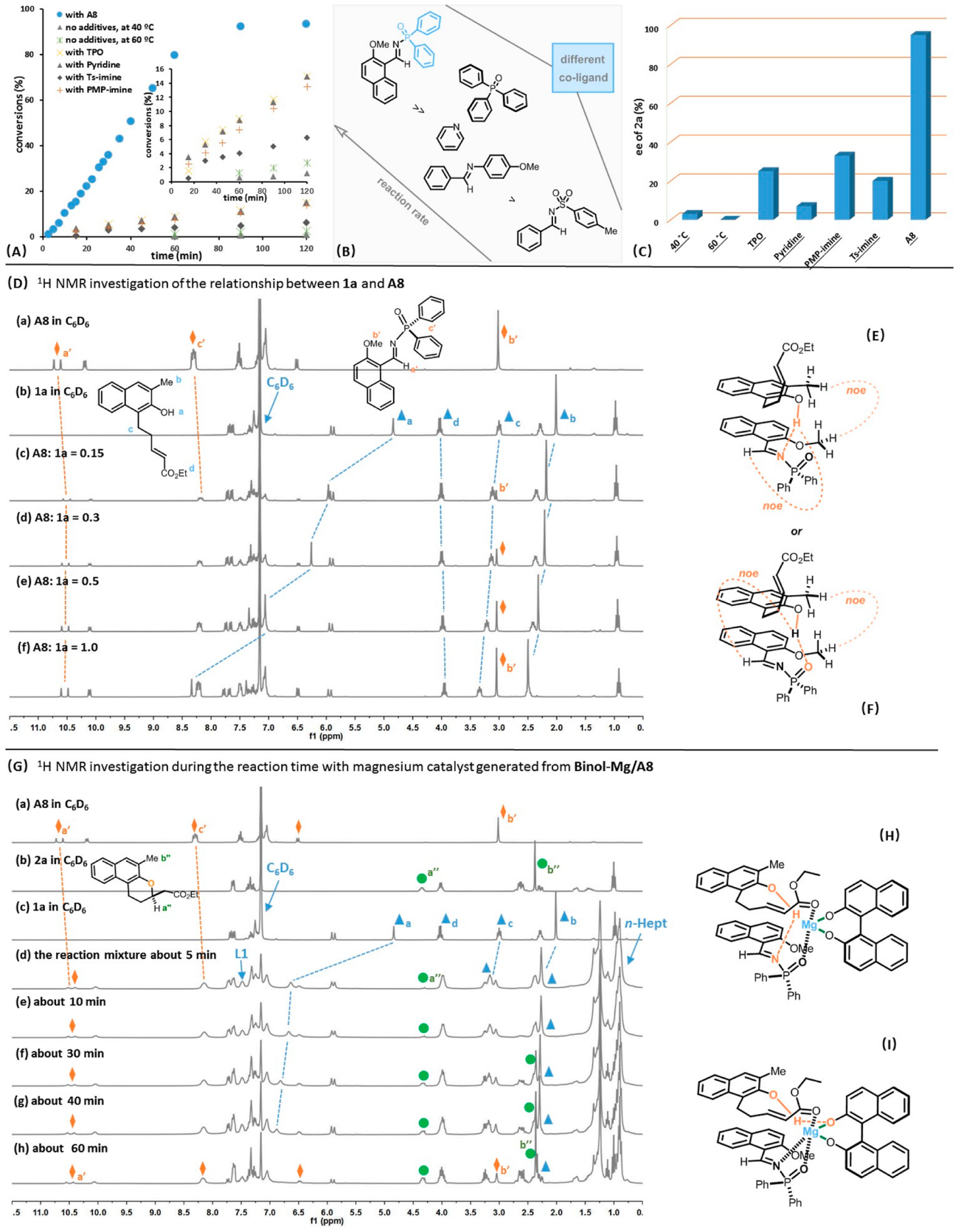

Figure 2. Further investigation of the imine cocatalyst functions. (A) Monitor of conversions with different coligands. (B) Formal comparison of the reaction rate under these coligands. (C) Enantioselectivity results with different coligands. (D) ^{1}H NMR analysis of the relationship between **1a** and **A8**. (E,F) NOESY analysis results of the mixture of **1a** and **A8**, and the complexes might form hydrogen bonds at different sites. (G) ^{1}H NMR investigation during the reaction time. (H,I) Proposed generation complexes between the catalyst and substrate **1a**, implying the deprotonation process might occur at different sites.

https://doi.org/10.1021/jacsau.3c00584
JACS Au 2024, 4, 164−176

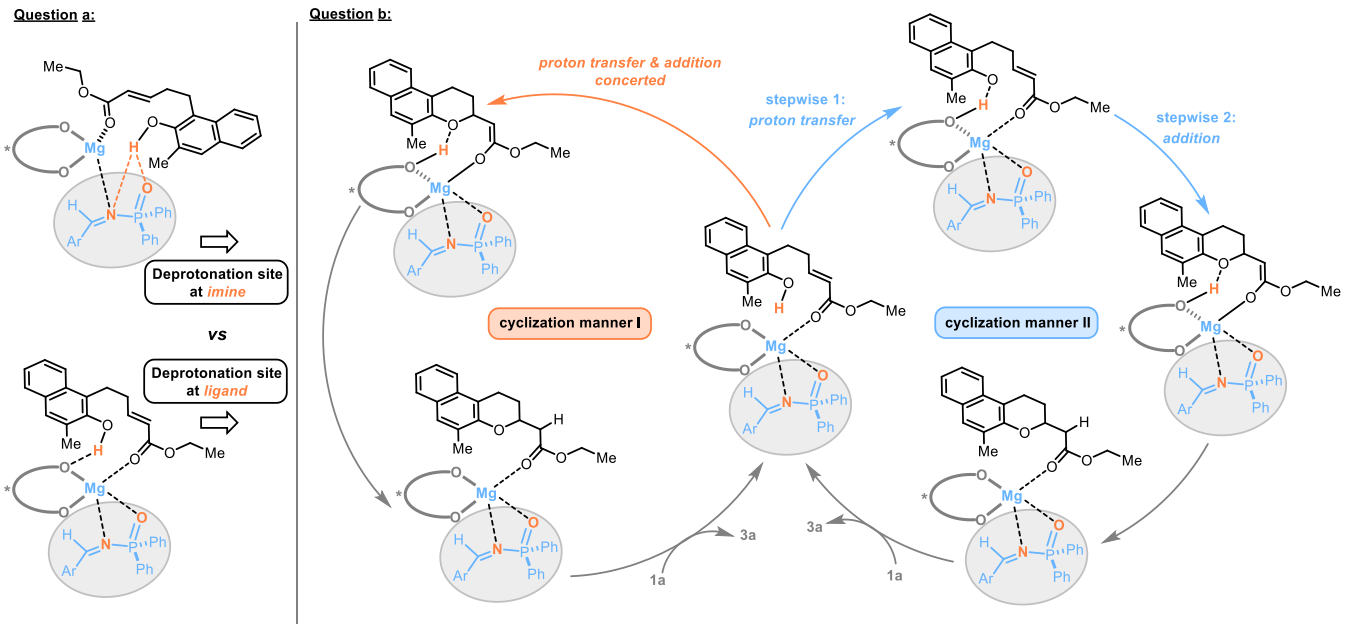

Figure 3. Possible mechanism of the reaction and the relative questions.

NMR investigations between **1a** and the catalyst **L1**/**Mg**/**A8**. In the situation of the relationship between **1a** and **A8**, downfield shift of the active phenol proton was clearly observed in the presence of **A8**, and a higher loading amount led to a substantial shift (Figure 2D).

The hydrogens on the adjacent carbon atoms b and c also undergo an unambiguous shift. For imine **A8**, several chemical shifts were also observed accordingly. Interestingly, by the analysis of the NOESY spectra of the admixture of **1a** and **A8** (1:1), phenol **1a** and imine coligand **A8** have intermolecular H−H interaction (Figure 2E,F, and the NOESY spectra in the Supporting Information). The ^{1}H NMR analysis also proved that the phenol itself cannot self-catalyze the oxa-Michael cyclization process. On the other hand, in the situation of the relationship between **1a** and the catalyst **L1**/**Mg**/**A8**, the chemical shifts were also observed for the hydrogens H_a, H_b, and H_c, and passivated peaks were generated for both **1a** and **A8**, which indicate the coordination results for these two compounds to **L1**/**Mg** accordingly (Figure 2G). Notably, the shift of the phenol active proton gradually moved downfield during the reaction's procedure, and the results might imply that the activation interaction between the substrate and the catalyst should be enhanced, or the coligand amount was passively increased along with the generation of the cyclization adduct. Given these mechanistic results, we speculated that the coligand might work with two possible roles in enhancing the efficiency of the oxa-Michael reaction: one is **A8** as a Brønsted base cocatalyzing the phenol bond to accelerate the cyclization process (Figure 2H); the other possibility is the enhancement of the basicity of the phenolic−Mg bond in the catalyst via coordination of these ligands, including the monodentate ligands such as pyridine or PMB-imine (Figure 2I). These two factors can synergistically promote the oxa-Michael reaction and meanwhile improve the enantioselectivities.

On the above experiments and mechanistic investigations, we can conclude that the Dpp-imine coligand can dramatically promote the activation of the phenol substrate as well as benefit the formation of an excellent chiral environment with the Binol/Mg complex. The plausible reaction mechanism is summarized in Figure 3. However, there exist two other questions awaiting further studies: (a) the deprotonation site in the catalytic complex; it can be a Dpp-imine coligand or the oxygen atom of Binol; and (b) the concreteness of the proton transfer and the cyclization addition process. The two processes may occur in either a stepwise or a concerted way. To answer these two basic questions and to shed more light on how imine coordination induces the chiral environment and affects the reaction mechanism, theoretical density functional theory (DFT) calculations coupled with high-level DLPNO−CCSD(T)/def2-TZVP energy calculations were performed.

The calculation utilized the single-metal coordination complex **R** (**L1**/**Mg**/**A8** = 1:1:1) as the starting point, which binds with 1 M of substrate **1a** to form a s complex **RC** (−21.0 kcal/mol). In the most plausible pathway leading to the major product, **RC** first undergoes an internal bond rotation in the substrate to give a relatively high-energy complex **RC-R^{Oa}**. In this process, the naphthyl group of the substrate rotates from a vertical orientation to a parallel orientation with regard to the imine plane. Next, a concerted base-assisted deprotonation/nucleophilic attack process, accompanied by tautomerization, occurs via the transition state **TS1-R^{Oa}** (−5.0 kcal/mol) with a barrier of 16.0 kcal/mol, leading to the magnesium enolate species **I1-R^{Oa}** (−9.0 kcal/mol). The base site was revealed to be one of the Binol oxygen site (labeled as **Oa** in Figure 4), whereas the other Binol oxygen (**Ob**) as the base site results into a higher-energy transition state (**TS1-R^{Ob}** in Figure 4A), largely due to the absence of π-stacking interactions between the substrate and the chiral pocket formed by the Mg/Binol/additive. Finally, the protonated Binol donated the proton back to the unsaturated carbon atom of the substrate via **TS2-R** (−2.4 kcal/mol) and yields the desired product. Throughout the reaction, Binol behaves as a "proton shuttle" to mediate the cyclization reaction.

In the calculation, we also located TSs corresponding to the pathway of proton deprotonation and nucleophilic attack step occurring in a stepwise manner, which involves **TS4-R^{Oa}** or **TS4-R^{Ob}** depending on which Binol oxygen acts as the base. The stepwise reaction channel is featured with a penta-coordinated

https://doi.org/10.1021/jacsau.3c00584
JACS Au 2024, 4, 164−176

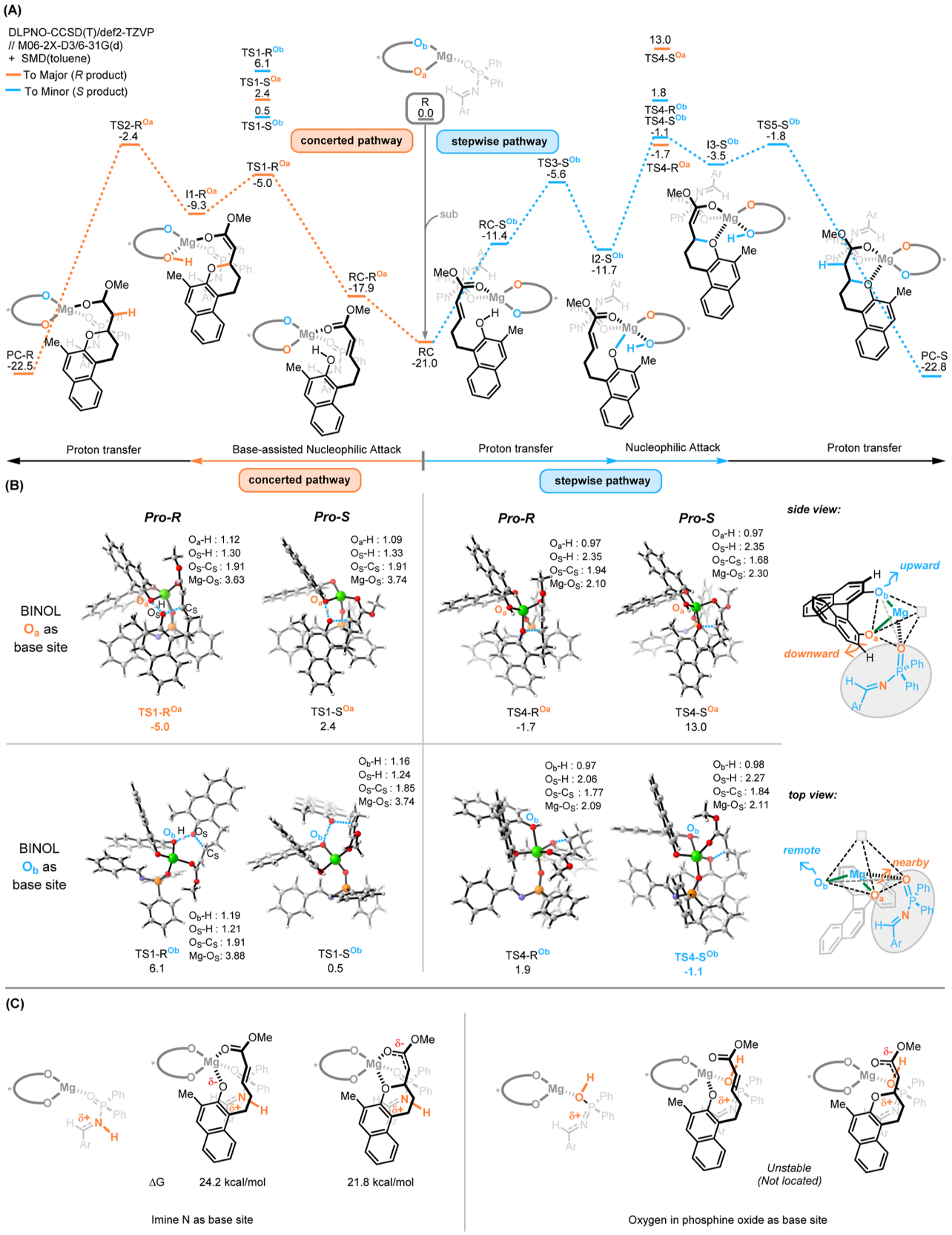

Figure 4. (A) Calculated reaction profile of the Mg-catalyzed oxa-Michael reaction. The possibility of either of the two Binol oxygen atoms (O_a and O_b) as proton shuttles was examined in the calculation. (B) Structure of key nucleophilic attack transition states and their relative free energies (in kcal/mol) to the energy reference. Distances are listed in Å and energy in kcal/mol. (C) Calculated intermediates with the substrate proton transferred to the imine N or the oxygen site in the phosphine oxide group.

https://doi.org/10.1021/jacsau.3c00584
JACS Au 2024, 4, 164−176

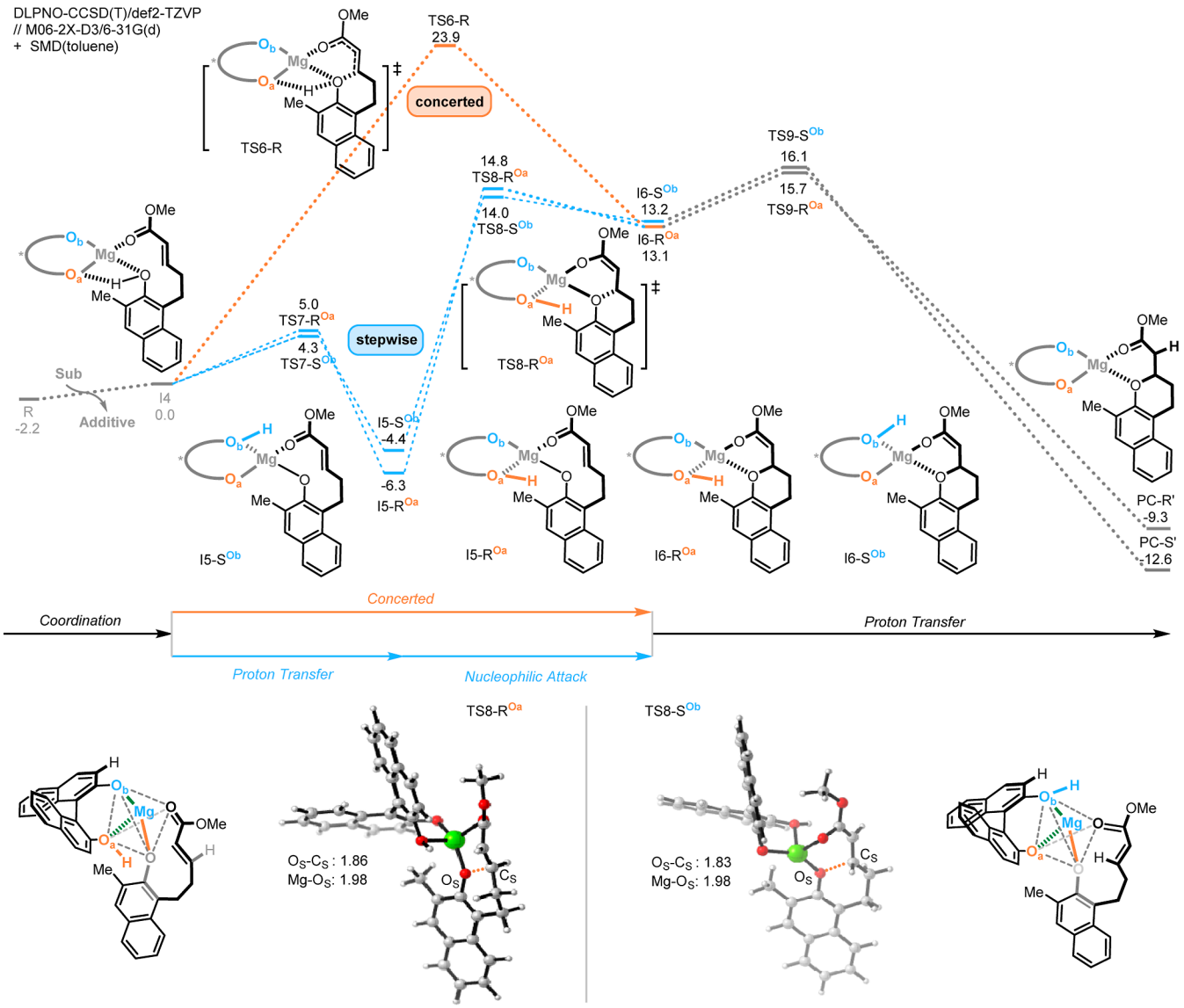

Figure 5. Calculated reaction pathway of Mg-catalyzed oxa-Michael reaction in the absence of the Dpp-imine coligand and structures of those key transition states.

magnesium phenolate intermediate, yielded from the deprotonation step. The followed nucleophilic attack step can take place either with the formed Binol hydroxyl group coordinating to (path A of penta-coordinated Mg) or dissociating from the metal center (path B of tetracoordinated Mg in Figure S4). Both stepwise pathways are calculated to involve transition states higher by at least 2.3 kcal/mol (TS4-R^{OaD} in Figure S4) than the concerted **TS1-R^{Oa}** (−5.0 kcal/mol). Notably, the concerted and stepwise deprotonation/nucleophilic attack pathways (via TS4-R^{OaD} or TS4-R^{Oa}) utilizing the same BINOL oxygen base site share the same TS (TS2-R^{Oa}) for the following turnover proton transfer process. Meanwhile, TS4-R^{Ob} of the stepwise pathway using the other BINOL oxygen as the base site is already much higher in energy (by 4.2 kcal/mol) than the rate-determining TS2-R^{Oa} of the most favorable pathway. Therefore, the reaction leading to the major enantiomer follows a concerted base-assisted deprotonation/nucleophilic attack mechanism.

In contrast, the most favorable pathway, leading to the minor *S*-configured enantiomer prefers the stepwise deprotonation/nucleophilic attack mechanism rather than the concerted mechanism. The concerted pathway shows a transition state (**TS1-S^{Ob}**) being 1.6 kcal/mol above in energy with respect to the rate-determining nucleophilic attack transition state (**TS4-S^{Ob}**) in the stepwise pathway. Compared with **TS1-R^{Oa}** and **TS2-R^{Oa}** leading to the major enantiomer, the turn over **TS4-S^{Ob}** leading to the minor enantiomer is higher in energy by >1.3 kcal/mol, which could well explain the excellent enantioselectivity of the current reaction. In the stepwise pathway leading to the S-configured product, the nucleophilic attack transition state with the Binol hydroxyl group dissociated from the metal center is higher in energy by ∼3.0 kcal/mol than the case (**TS4-S^{Ob}**) of Binol hydroxyl group coordinating with the Mg(II) center.

Additionally, we have examined the possibility of proton transfer to the imine N site or oxygen in the phosphine oxide group (Figure 4C). The calculation revealed that imine N as the base site results into high-energy charge separation intermediates, while structures with the protonated phosphine oxide could not be located as minimum on the potential energy surface. Thus, the possibility of imine N or oxygen site in the phosphine oxide group as the base site can be faithfully excluded.

https://doi.org/10.1021/jacsau.3c00584
JACS Au 2024, 4, 164−176

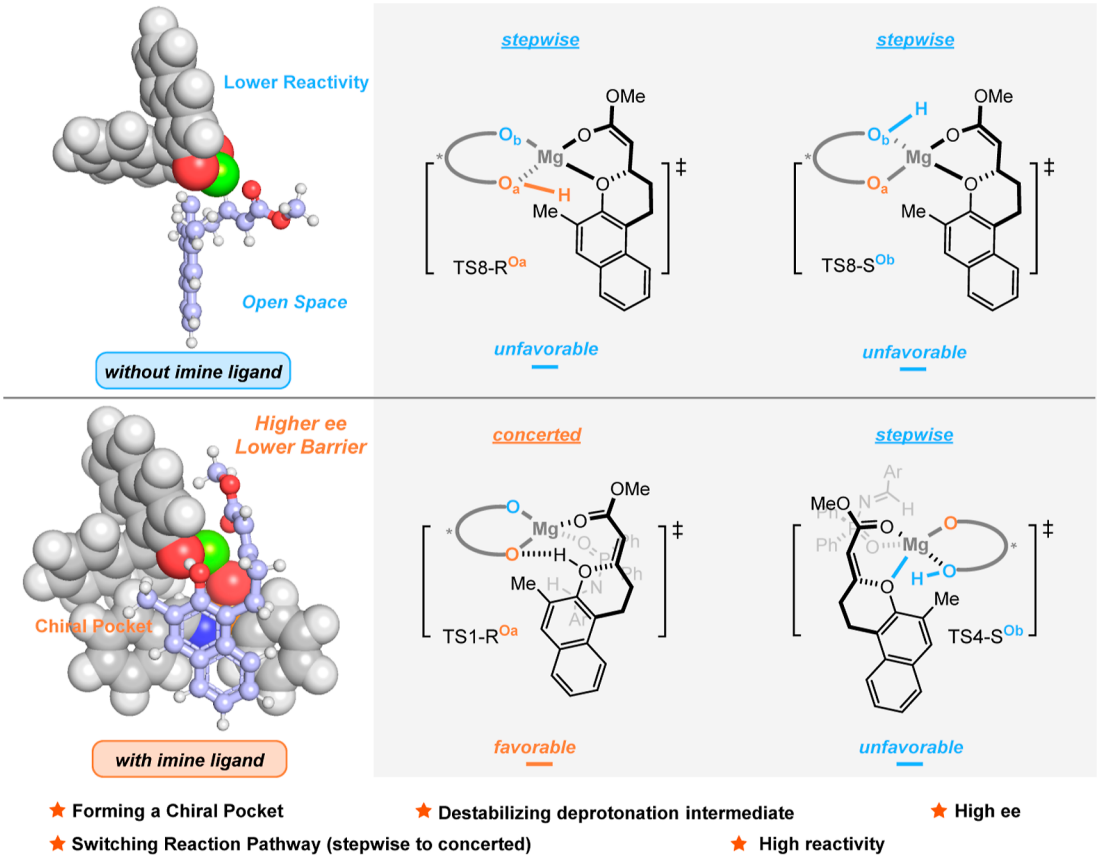

Figure 6. Summary of the role of additive in the reaction. Mg/Binol/additive complex is shown in spheres, while the substrate is shown in sticks.

To gain more insights into the crucial factors responsible for the excellent enantioselectivity, analysis using the interaction/distortion energy decomposition model and the independent gradient model based on the Hirshfeld partition (IGMH) method was performed for those key reactant complexes (Figure S2). A close look at those RC structures and their energies clearly revealed that Mg/Binol/additive forms a perfect chiral pocket to bind the substrate in a selective way. **RC-R^{Oa}**, the prereaction complex of **TS1-R^{Oa}**, is 2.8 and 6.6 kcal/mol lower in energy than **RC-S^{Oa}** and **RC-S^{Ob}**, respectively. **RC-S^{Oa}** and **RC-S^{Ob}** are the prereaction complexes, leading to the minor *S*-configured enantiomer and utilizing different BINOL oxygen sites as bases. Distortion/interaction analysis suggested that the energy difference of those RCs mainly comes from the interaction energy difference between the substrate and the Mg/Binol/additive complex, though structure distortion also contributes (Figure S2). The IGMH plot revealed that in **RC-R^{Oa}**, the substrate shows more pairs of van der Waals interactions with the Mg/Binol/additive complex, in particular interactions between the ester group and the Binol aromatic ring, while **RC-S^{Oa}** and **RC-S^{Ob}** exhibit less pronounced intermolecular interactions. These observations indicate that the chiral pocket formed by Mg/Binol/additive favors the binding and interaction of the *pro-R* substrate, which is believed to be responsible for the excellent enantioselectivity.

To explore more details concerning the role of the additive, we performed additional calculations for the additive-free reaction (Figure 5). The results showed that, without the additive, both of the favorable pathways leading to the *S*- or *R*-configured product prefer the stepwise deprotonation/nucleophilic attack pathway, while the concerted pathway is much higher in energy. Importantly, the most plausible reaction pathway in the absence of the additive shows a higher barrier by ca. 3 kcal/mol than the case with the additive. The main reason for this barrier increment can be attributed to the formation of a relatively stable/inactive deprotonation intermediate (**I5-R^{Oa}**), which is ∼6.3 kcal/mol lower in energy than the reactant complex. Charge analysis revealed that the phenolate oxygen in **I5-R^{Oa}** is more charge-deficient (−0.749 e), and thus a poorer nucleophile, than that in the additive-present deprotonation intermediate (−0.767 e in **I4-R^{Oa}**). As a result, nucleophilic attack in the absence of the additive exhibits a relatively higher barrier. This is in accordance with the experimental observation that introducing an additive accelerates the reaction. Besides, in the absence of the additive, the overall barrier leading to the *R*-(22.0 kcal/mol) or *S*- (22.4 kcal/mol) configured product is comparable, since Mg/Binol could not form a chiral pocket (Figure 5) to discriminate transition states in the *pro-R* and *pro-S* conformation. This reinforces our conclusion of the formation of a chiral pocket in the presence of the imine additive.

These experimental and theoretical results indicate three unique roles of the additive (Figure 6). First, the additive, together with the chiral Binol-coordinated Mg, forms a chiral pocket to favor the binding and reaction of the substrate in the *pro-R* conformation. Second, the coordination of the imine additive could modulate the stabilization effect of the metal on the forming negatively charged phenolate oxygen site and avoid the formation of a stable/inactive deprotonation intermediate. This effect could account for the rate enhancement when introducing an additive in the reaction. Third, the microenvironment formed by Mg/Binol/additive favors the deprotonation and nucleophilic attack steps of the *pro-R* substrate

https://doi.org/10.1021/jacsau.3c00584
JACS Au 2024, 4, 164−176

completed in a concerted pathway, rather than the stepwise pathways that are followed by the additive-free catalyst. This indicates the role of the additive in switching the reaction channel. These three factors are expected to account for the experimental results that the reaction in the presence of an additive shows a better enantioselectivity and a higher reactivity than the additive-free reaction.

CONCLUSIONS

In summary, we have successfully identified Dpp-imine as the powerful coligand in the magnesium-catalyzed intramolecular oxa-Michael reaction. This active imine ligand can not only create an excellent chiral environment with an intense nonsymmetrical pocket but also dramatically enhance the efficiency of the cyclization reaction by switching the stepwise pathway to a concerted process, in which the deprotonation and cyclization addition progress show a lower energy requirement. A series of mechanistic investigation experiments and DFT calculation results support the aforementioned conclusion. This work will stimulate more research works to extend the role of active imines as ligands beyond the conventional substrate model in former studies. Our further work on Dpp-imine coligand for other magnesium-based catalytic reactions is ongoing, and we will apply this novel catalytic strategy in more asymmetric reactions.

METHODS

Typical Procedure for the Magnesium-Catalyzed Cyclization Reaction

To a stirred solution of **L1** (8.58 mg, 0.03 mmol) in toluene (0.4 mL) was added Bu_2Mg (30 μ L, 1.0 M in heptane, 0.03 mmol) under an argon atmosphere. After the mixture was stirred at room temperature for 30 min, **1** (0.20 mmol) and **A8** (0.06 mmol) in toluene (0.6 mL) were added. Then, the reaction was stirred at 40 °C overnight. Then, it was cooled to 0 °C, and dry methanol (0.2 mL) and $NaBH_4$ (7.6 mg) were added, and the reaction was quenched with saturated NH_4Cl; then, the reaction was extracted three times with DCM. The combined organic layers were dried over Na_2SO_4 and concentrated under vacuum, and the product was purified by column chromatography to obtain the cyclization adducts.

Note: the introduction of $NaBH_4$ makes the column chromatography process easier to remove the aldehyde, which is generated from the decomposition of DPP-imine **A8**.

ASSOCIATED CONTENT

Supporting Information

The Supporting Information is available free of charge at https://pubs.acs.org/doi/10.1021/jacsau.3c00584.

Synthetic procedures, NMR and HPLC spectra, calculation details, and crystallographic data (PDF)

AUTHOR INFORMATION

Corresponding Authors

Xiaoyong Zhang − *Institute of Systems and Physical Biology, Shenzhen Bay Laboratory, Shenzhen 518055, P. R. China;* orcid.org/0000-0002-0966-4343; Email: zhangxyleuven@gmail.com

Linqing Wang − *Key Laboratory of Preclinical Study for New Drugs of Gansu Province, School of Basic Medical Sciences & Research Unit of Peptide Science, 2019RU066, Lanzhou University, Lanzhou 730000 Gansu, P. R. China;* orcid.org/0000-0001-5922-1332; Email: lqwang@lzu.edu.cn

Dongxu Yang − *Key Laboratory of Preclinical Study for New Drugs of Gansu Province, School of Basic Medical Sciences & Research Unit of Peptide Science, 2019RU066, Lanzhou University, Lanzhou 730000 Gansu, P. R. China;* orcid.org/0000-0002-8993-5245; Email: yangdx@lzu.edu.cn

Authors

Yingfan Xu − *Key Laboratory of Preclinical Study for New Drugs of Gansu Province, School of Basic Medical Sciences & Research Unit of Peptide Science, 2019RU066, Lanzhou University, Lanzhou 730000 Gansu, P. R. China*

Dan Liu − *Institute of Systems and Physical Biology, Shenzhen Bay Laboratory, Shenzhen 518055, P. R. China;* orcid.org/0000-0001-5888-7933

Feiyun Gao − *Key Laboratory of Preclinical Study for New Drugs of Gansu Province, School of Basic Medical Sciences & Research Unit of Peptide Science, 2019RU066, Lanzhou University, Lanzhou 730000 Gansu, P. R. China*

Shixin Li − *Key Laboratory of Preclinical Study for New Drugs of Gansu Province, School of Basic Medical Sciences & Research Unit of Peptide Science, 2019RU066, Lanzhou University, Lanzhou 730000 Gansu, P. R. China*

Complete contact information is available at: https://pubs.acs.org/10.1021/jacsau.3c00584

Author Contributions

[§]Y.X. and D.L. contributed equally on this work. D.Y. conceived the study. D.Y., L.W., and X.Z. directed and supervised the research. Y.X. and L.W. performed the synthesized experiments and analyzed the data. D.L. and X.Z. performed the DFT calculation experiments. All authors discussed the results and prepared the manuscript and Supporting Information.

Notes

The authors declare no competing financial interest.

ACKNOWLEDGMENTS

We acknowledge the financial support from the Innovation Fund for Medical Sciences (CIFMS, 2019-I2M-5-074, 2021-I2M-1-026, 2021-I2M-3-001), the Fundamental Research Funds for the Central Universities (lzujbky-2022-ey11, lzujbky-2022-40), the Funding from Guangdong Basic and Applied Basic Research Foundation (2022A1515110835), the LongYuan Young Talents Program, and the Funds for Fundamental Research Creative Groups of Gansu Province (20JR5RA310).

REFERENCES

(1) For recent reviews on imine as substrates in chemical synthesis: Verkade, J. M. M.; Hemert, L. J. C.; Quaedflieg, P. J. L. M.; Rutjes, F. P. J. T. Organocatalysed Asymmetric Mannich Reactions. *Chem. Soc. Rev.* **2008**, *37*, 29−41.

(2) Arrayás, R. G.; Carretero, J. C. Catalytic asymmetric direct Mannich reaction: a powerful tool for the synthesis of α,β-diamino acids. *Chem. Soc. Rev.* **2009**, *38*, 1940−1948.

(3) Noble, A.; Anderson, J. C. Nitro-Mannich Reaction. *Chem. Rev.* **2013**, *113*, 2887−2939.

(4) Belowich, M. E.; Stoddart, J. F. Dynamic Imine Chemistry. *Chem. Soc. Rev.* **2012**, *41*, 2003−2024.

(5) Foubelo, F.; Yus, M. Diastereoselective Indium-Promoted Allylation of ChiralN-Sulfinyl Imines. *Eur. J. Org Chem.* **2014**, *2014*, 485−491.
(6) Huo, H.-X.; Duvall, J. R.; Huang, M. Y.; Hong, R. Catalytic Asymmetric Allylation of Carbonyl Compounds and Imines with Allylic Boronates. *Org. Chem. Front.* **2014**, *1*, 303−320.
(7) Vesely, J.; Rios, R. Enantioselective Methodologies Using N-Carbamoyl-Imines. *Chem. Soc. Rev.* **2014**, *43*, 611−630.
(8) Dong, H.-Q.; Xu, M.-H.; Feng, C.-G.; Sun, X.-W.; Lin, G.-Q. Recent Applications of Chiral N-tert-Butanesulfinyl Imines, Chiral Diene Ligands and Chiral Sulfur-Olefin Ligands in Asymmetric Synthesis. *Org. Chem. Front.* **2015**, *2*, 73−89.
(9) Reid, J. P.; Simon, L.; Goodman, J. M. A Practical Guide for Predicting the Stereochemistry of Bifunctional Phosphoric Acid Catalyzed Reactions of Imines. *Acc. Chem. Res.* **2016**, *49*, 1029−1041.
(10) Chen, D.; Xu, M.-H. Transition Metal-Catalyzed Asymmetric Addition of Organoboron Reagents to Imines. *Chin. J. Org. Chem.* **2017**, *37*, 1589−1612.
(11) Saha, S. K.; Bera, A.; Singh, S.; Rana, N. K. Asymmetric Catalytic Approaches Employing α, β-Unsaturated Imines. *Eur. J. Org Chem.* **2023**, *26*, No. e202201470.
(12) Wang, L.; Yang, D. Take Advantage of the N-Nucleophilicity of Imine in Catalytic Cyclization Reactions. *ChemCatChem* **2023**, *15*, No. e202300189.
(13) Liu, Q.-L.; Chen, W.; Jiang, Q.-Y.; Bai, X.-F.; Li, Z.; Xu, Z.; Xu, L.-W. A D-Camphor-Based Schiff Base as a Highly Efficient N,P Ligand for Enantioselective Palladium-Catalyzed Allylic Substitutions. *ChemCatChem* **2016**, *8*, 1495−1499.
(14) De, S.; Jain, A.; Barman, P. Recent Advances in the Catalytic Applications of Chiral Schiff-Base Ligands and Metal Complexes in Asymmetric Organic Transformations. *ChemistrySelect* **2022**, *7*, No. e202104334.
(15) Yuan, Y.; Li, X.; Sun, J.; Ding, K. To Probe the Origin of Activation Effect of Carboxylic Acid and (+)-NLE in Tridentated Titanium Catalyst Systems. *J. Am. Chem. Soc.* **2002**, *124*, 14866−14867.
(16) Du, H.; Ding, K. Enantioselective Catalysis of Hetero Diels-Alder Reaction and Diethylzinc Addition Using a Single Catalyst. *Org. Lett.* **2003**, *5*, 1091−1093.
(17) Matsubara, R.; Nakamura, Y.; Kobayashi, S. Highly Diastereo- and Enantioselective Reactions of Enecarbamates with Ethyl Glyoxylate to Give Optically Active syn and anti α-Alkyl-β-Hydroxy Imines and Ketones. *Angew. Chem., Int. Ed.* **2004**, *43*, 3258−3260.
(18) Chen, C.; Hong, L.; Xu, Z.-Q.; Liu, L.; Wang, R. Low Ligand Loading, Highly Enantioselective Addition of Phenylacetylene to Aromatic Ketones Catalyzed by Schiff-Base Amino Alcohols. *Org. Lett.* **2006**, *8*, 2277−2280.
(19) Zhang, Y.-Z.; Zhu, S.-F.; Wang, L.-X.; Zhou, Q.-L. Copper-Catalyzed Highly Enantioselective Carbenoid Insertion into Si—H Bonds. *Angew. Chem., Int. Ed.* **2008**, *47*, 8496−8498.
(20) Jiang, J.-J.; Huang, J.; Wang, D.; Zhao, M.-X.; Wang, F.-J.; Shi, M. Cu(I)-catalyzed asymmetric α-hydroxylation of β-keto esters in the presence of chiral phosphine-Schiff base-type ligands. *Tetrahedron: Asymmetry* **2010**, *21*, 794−799.
(21) Su, Z.; Qin, S.; Hu, C.; Feng, X. Theoretical Investigations on the Mechanism of Hetero-Diels-Alder Reactions of Brassards Diene and 1, 3-Butadiene Catalyzed by a Tridentate Schiff Base Titanium(IV) Complex. *Chem.—Eur. J.* **2010**, *16*, 4359−4367.
(22) Yang, W.; Du, D.-M. Highly Enantioselective Henry Reaction Catalyzed by C2-Symmetric Modular BINOL-Oxazoline Schiff Base Copper(II) Complexes Generated in Situ. *Eur. J. Org Chem.* **2011**, *2011*, 1552−1556.
(23) Rahman, M. A.; Cellnik, T.; Ahuja, B. B.; Li, L.; Healy, A. R. A Catalytic Enantioselective Stereodivergent Aldol Reaction. *Sci. Adv.* **2023**, *9*, No. eadg8776.
(24) Yoon, T. P.; Jacobsen, E. N. Highly Enantioselective Thiourea-Catalyzed Nitro-Mannich Reactions. *Angew. Chem., Int. Ed.* **2005**, *44*, 466−468.
(25) Yoshida, T.; Morimoto, H.; Kumagai, N.; Matsunaga, S.; Shibasaki, M. Non-C2-Symmetric, Chirally Economical, and Readily Tunable Linked-binols: Design and Application in a Direct Catalytic Asymmetric Mannich-Type Reaction. *Angew. Chem., Int. Ed.* **2005**, *44*, 3470−3474.
(26) Carswell, E. L.; Snapper, M. L.; Hoveyda, A. H. A Highly Efficient and Practical Method for Catalytic Asymmetric Vinylogous Mannich (AVM) Reactions. *Angew. Chem., Int. Ed.* **2006**, *45*, 7230−7233.
(27) Han, Z.; Wang, Z.; Zhang, X.; Ding, K. Spiro[4,4]-1,6-Nonadiene-Based Phosphine-Oxazoline Ligands forIridium-Catalyzed Enantioselective Hydrogenation of Ketimines. *Angew. Chem., Int. Ed.* **2009**, *48*, 5345−5349.
(28) Zhou, C.-Y.; Zhu, S.-F.; Wang, L.-X.; Zhou, Q.-L. Enantioselective Nickel-Catalyzed Reductive Coupling of Alkynes and Imines. *J. Am. Chem. Soc.* **2010**, *132*, 10955−10957.
(29) Kano, T.; Song, S.; Kubota, Y.; Maruoka, K. Highly Diastereo- and Enantioselective Mannich Reactions of Synthetically Flexible Ketimines with Secondary Amine Organocatalysts. *Angew. Chem., Int. Ed.* **2012**, *51*, 1191−1194.
(30) Zhang, W.-Q.; Cheng, L.-F.; Yu, J.; Gong, L.-Z. A Chiral Bis(betaine) Catalyst for the Mannich Reaction of Azlactones and Aliphatic Imines. *Angew. Chem., Int. Ed.* **2012**, *51*, 4085−4088.
(31) Wang, Q.; Leutzsch, M.; van Gemmeren, M.; List, B. Disulfonimide-Catalyzed Asymmetric Synthesis of β3-Amino Esters Directly from N-Boc-Amino Sulfones. *J. Am. Chem. Soc.* **2013**, *135*, 15334−15337.
(32) Liu, X.; Meng, Z.; Li, C.; Lou, H.; Liu, L. Organocatalytic Enantioselective Oxidative C—H Alkenylation and Arylation of *N*-Carbamoyl Tetrahydropyridines and Tetrahydro-β-carbolines. *Angew. Chem., Int. Ed.* **2015**, *54*, 6012−6015.
(33) Wang, Y.; Mo, M.; Zhu, K.; Zheng, C.; Zhang, H.; Wang, W.; Shao, Z. Asymmetric synthesis of syn-propargylamines and unsaturated β-amino acids under Brønsted base catalysis. *Nat. Commun.* **2015**, *6*, 8544−8552.
(34) Wang, Y.; Jiang, L.; Li, L.; Dai, J.; Xiong, D.; Shao, Z. An Arylation Strategy to Propargylamines: Catalytic Asymmetric Friedel-Crafts-type Arylation Reactions of C-Alkynyl Imines. *Angew. Chem., Int. Ed.* **2016**, *55*, 15142−15146.
(35) You, Y.; Zhang, L.; Cui, L.; Mi, X.; Luo, S. Catalytic Asymmetric Mannich Reaction with N-Carbamoyl Imine Surrogates of Formaldehyde and Glyoxylate. *Angew. Chem., Int. Ed.* **2017**, *56*, 13814−13818.
(36) Zhang, H.-J.; Shi, C.-Y.; Zhong, F.; Yin, L. Direct Asymmetric Vinylogous and Bisvinylogous Mannich-Type Reaction Catalyzed by a Copper(I) Complex. *J. Am. Chem. Soc.* **2017**, *139*, 2196−2199.
(37) Zhang, F.; Dai, X.; Dai, L.; Zheng, W.; Chan, W.-L.; Tang, X.; Zhang, X.; Lu, Y. Phosphine-Catalyzed Enantioselective (3 + 2) Annulation of Vinylcyclopropanes with Imines for the Synthesis of Chiral Pyrrolidines. *Angew. Chem., Int. Ed.* **2022**, *61*, No. e2022032.
(38) Chen, P.; Tan, S.-Z.; Zhu, L.; Ouyang, Q.; Jia, Z.-J.; Du, W.; Chen, Y.-C. Palladium-Catalyzed Inverse and Normal Dehydrogenative Aza-Morita-Baylis-Hillman Reactions with γ,δ-Unsaturated Compounds. *Angew. Chem., Int. Ed.* **2023**, *62*, No. e202301519.
(39) Xu, J.; Song, Y.; Yang, J.; Yang, B.; Su, Z.; Lin, L.; Feng, X. Sterically Hindered and Deconjugative α-Regioselective Asymmetric Mannich Reaction of Meinwald Rearrangement-Intermediate. *Angew. Chem., Int. Ed.* **2023**, *62*, No. e202217887.
(40) Yang, D.; Wang, L.; Li, D.; Wang, R. Magnesium Catalysis in Asymmetric Synthesis. *Chem.* **2019**, *5*, 1108−1166.
(41) Yang, D.; Wang, L. Strategies of In Situ Generated Magnesium Catalysis in Asymmetric Reactions. *Synlett* **2021**, *32*, 1309−1315.
(42) Du, H.; Zhang, X.; Wang, Z.; Bao, H.; You, T.; Ding, K. BINOLate-Magnesium Catalysts for Enantioselective Hetero-Diels-Alder Reaction of Danishefsky's Diene with Aldehydes. *Eur. J. Org Chem.* **2008**, *2008*, 2248−2254.
(43) Yoshino, T.; Morimoto, H.; Lu, G.; Matsunaga, S.; Shibasaki, M. Construction of contiguous tetrasubstituted chiral carbon stereocenters via direct catalytic asymmetric Aldol reaction of alpha-isothiocyanato esters with ketones. *J. Am. Chem. Soc.* **2009**, *131*, 17082−17083.
(44) Hatano, M.; Horibe, T.; Ishihara, K. Magnesium(II)-Binaphtholate as a Practical Chiral Catalyst for the Enantioselective

https://doi.org/10.1021/jacsau.3c00584
JACS Au 2024, 4, 164−176

Direct Mannich-Type Reaction with Malonates. *Org. Lett.* **2010**, *12*, 3502−3505.
(45) Hatano, M.; Horibe, T.; Ishihara, K. Chiral Magnesium(II) Binaphtholates as Cooperative Brønsted/Lewis Acid-Base Catalysts for the Highly Enantioselective Addition of Phosphorus Nucleophiles to α,β-Unsaturated Esters and Ketones. *Angew. Chem., Int. Ed.* **2013**, *52*, 4549−4553.
(46) Yang, D.; Wang, L.; Han, F.; Zhao, D.; Zhang, B.; Wang, R. Direct Site-Specific and Highly Enantioselective γ-Functionalization of Linear α,β-Unsaturated Ketones: Bifunctional Catalytic Strategy. *Angew. Chem., Int. Ed.* **2013**, *52*, 6739−6742.
(47) Yang, D.; Wang, L.; Han, F.; Li, D.; Zhao, D.; Wang, R. Intermolecular Enantioselective Dearomatization Reaction of β-Naphthol Using meso-Aziridine: A Bifunctional In Situ Generated Magnesium Catalyst. *Angew. Chem., Int. Ed.* **2015**, *54*, 2185−2189.
(48) Yang, D.; Wang, L.; Kai, M.; Li, D.; Yao, X.; Wang, R. Application of a C—C Bond-Forming Conjugate Addition Reaction in Asymmetric Dearomatization of β-Naphthols. *Angew. Chem., Int. Ed.* **2015**, *54*, 9523−9527.
(49) Hatano, M.; Nishikawa, K.; Ishihara, K. Enantioselective Cycloaddition of Styrenes with Aldimines Catalyzed by a Chiral Magnesium Potassium Binaphthyldisulfonate Cluster as a Chiral Brønsted Acid Catalyst. *J. Am. Chem. Soc.* **2017**, *139*, 8424−8427.
(50) Wang, L.; Yang, D.; Li, D.; Liu, X.; Wang, P.; Wang, K.; Zhu, H.; Bai, L.; Wang, R. The Important Role of the Byproduct Triphenylphosphine Oxide in the Magnesium(II)-Catalyzed Enantioselective Reaction of Hemiacetals and Phosphorus Ylides. *Angew. Chem., Int. Ed.* **2018**, *57*, 9088−9092.
(51) Li, D.; Yang, Y.; Zhang, M.; Wang, L.; Xu, Y.; Yang, D.; Wang, R. Activation of Allylic Esters in an Intramolecular Vinylogous Kinetic Resolution Reaction with Synergistic Magnesium Catalysts. *Nat. Commun.* **2020**, *11*, 2559−2568.
(52) Xu, P.; Shen, C.; Xu, A.; Low, K.-H.; Huang, Z. Desymmetric Cyanosilylation of Acyclic 1,3-Diketones. *Angew. Chem., Int. Ed.* **2022**, *61*, No. e20220844.
(53) Wang, L.; Zhu, H.; Peng, T.; Xu, Y.; Hou, Y.; Li, S.; Pang, S.; Zhang, H.; Yang, D. A Tandem Asymmetric Oxidation-oxa-Michael Sequence for Dearomatization of β-Naphthols. *Chin. Chem. Lett.* **2022**, *33*, 4273−4276.
(54) Wang, L.; Gao, F.; Zhang, X.; Peng, T.; Xu, Y.; Wang, R.; Yang, D. Concerted Enantioselective [2 + 2] Cycloaddition Reaction of Imines Mediated by a Magnesium Catalyst. *J. Am. Chem. Soc.* **2023**, *145*, 610−625.
(55) Wang, P.-S.; Liu, P.; Zhai, Y.-J.; Lin, H.-C.; Han, Z.-Y.; Gong, L.-Z. Asymmetric Allylic C-H Oxidation for the Synthesis of Chromans. *J. Am. Chem. Soc.* **2015**, *137*, 12732−12735.
(56) Ammann, E.; Liu, W.; White, M. C. Enantioselective Allylic C-H Oxidation of Terminal Olefins to Isochromans by Palladium(II)/Chiral Sulfoxide Catalysis. *Angew. Chem., Int. Ed.* **2016**, *55*, 9571−9575.
(57) Liu, L.; Kaib, P. S. J.; Tap, A.; List, B. A General Catalytic Asymmetric Prins Cyclization. *J. Am. Chem. Soc.* **2016**, *138*, 10822−10825.
(58) Wan, M.; Sun, S.; Li, Y.; Liu, L. Organocatalytic Redox Deracemization of Cyclic Benzylic Ethers Enabled by An Acetal Pool Strategy. *Angew. Chem., Int. Ed.* **2017**, *56*, 5116−5120.
(59) Schafroth, M. A.; Rummelt, S. M.; Sarlah, D.; Carreira, E. M. Enantioselective Iridium-Catalyzed Allylic Cyclizations. *Org. Lett.* **2017**, *19*, 3235−3238.
(60) Wang, Y.; Zhang, W.-Y.; You, S.-L. Ketones and Aldehydes as O-Nucleophiles in Iridium-Catalyzed Intramolecular Asymmetric Allylic Substitution Reaction. *J. Am. Chem. Soc.* **2019**, *141*, 2228−2232.
(61) Sun, S.; Yang, Y.; Zhao, R.; Zhang, D.; Liu, L. Site- and Enantio differentiating C(sp3)-H Oxidation Enables Asymmetric Access to Structurally and Stereochemically Diverse Saturated Cyclic Ethers. *J. Am. Chem. Soc.* **2020**, *142*, 19346−19353.
(62) Nising, C. F.; Bräse, S. The oxa-Michael Reaction: from Recent Developments to Applications in Natural Product Synthesis. *Chem. Soc. Rev.* **2008**, *37*, 1218−1228.
(63) Nising, C. F.; Bräse, S. Recent Developments in the Field of oxa-Michael Reactions. *Chem. Soc. Rev.* **2012**, *41*, 988−999.
(64) Wang, Y.; Du, D.-M. Recent Advances in Organocatalytic Asymmetric oxa-Michael Addition Triggered Cascade Reactions. *Org. Chem. Front.* **2020**, *7*, 3266−3283.
(65) Sun, S.; Ma, Y.; Liu, Z.; Liu, L. Oxidative Kinetic Resolution of Cyclic Benzylic Ethers. *Angew. Chem., Int. Ed.* **2021**, *60*, 176−180.
(66) Gu, Q.; Rong, Z.-Q.; Zheng, C.; You, S.-L. Desymmetrization of Cyclohexadienones via Brønsted Acid-Catalyzed Enantioselective Oxo-Michael Reaction. *J. Am. Chem. Soc.* **2010**, *132*, 4056−4057.
(67) Asano, K.; Matsubara, S. Asymmetric Catalytic Cycloetherification Mediated by Bifunctional Organocatalysts. *J. Am. Chem. Soc.* **2011**, *133*, 16711−16713.
(68) Kobayashi, Y.; Taniguchi, Y.; Hayama, N.; Inokuma, T.; Takemoto, Y. A Powerful Hydrogen-Bond-Donating Organocatalyst for theEnantioselective Intramolecular Oxa-Michael Reaction of α,β-Unsaturated Amides and Esters. *Angew. Chem., Int. Ed.* **2013**, *52*, 11114−11118.
(69) Yoneda, N.; Fujii, Y.; Matsumoto, A.; Asano, K.; Matsubara, S. Organocatalytic Enantio- and Diastereoselective Cycloetherification via Dynamic Kinetic Resolution of Chiral Cyanohydrins. *Nat. Commun.* **2017**, *8*, 1397−1403.
(70) Sun, Z.; Zha, T.; Shao, Z. Enantiodivergent Synthesis of Tricyclic Chromans: Remote Nucleophilic Groups Switch Selectivity in Catalytic Asymmetric Cascade Reactions of Trifunctional Substrates. *Green Synth. Catal.* **2021**, *2*, 241−245.
(71) Zhu, D.-X.; Liu, J.-G.; Xu, M.-H. Stereodivergent Synthesis of Enantioenriched 2,3-Disubstituted Dihydrobenzofurans via a One-Pot C-H Functionalization/OxaMichael Addition Cascade. *J. Am. Chem. Soc.* **2021**, *143*, 8583−8589.
(72) Su, G.; Formica, M.; Yamazaki, K.; Hamlin, T. A.; Dixon, D. J. Catalytic Enantioselective Intramolecular Oxa-Michael Reaction to α,β-Unsaturated Esters and Amides. *J. Am. Chem. Soc.* **2023**, *145*, 12771−12782.
(73) Zheng, K.; Liu, X.; Feng, X. Recent Advances in Metal-Catalyzed Asymmetric 1,4-ConjugateAddition (ACA) of Nonorganometallic Nucleophiles. *Chem. Rev.* **2018**, *118*, 7586−7656.
(74) Chen, L.; Pu, M.; Li, S.; Sang, X.; Liu, X.; Wu, Y.-D.; Feng, X. Enantioselective Synthesis of Nitriles Containing a Quaternary Carbon Center by Michael Reactions of Silyl Ketene Imines with 1-Acrylpyrazoles. *J. Am. Chem. Soc.* **2021**, *143*, 19091−19098.
(75) Li, Y.; Xin, S.; Weng, R.; Liu, X.; Feng, X. Asymmetric Synthesis of Chromanone Lactones via Vinylogous Conjugate Addition of Butenolide to 2-Ester Chromones. *Chem. Sci.* **2022**, *13*, 8871−8875.
(76) Li, E.; Chen, J.; Huang, Y. Enantioselective Seleno-Michael Addition Reactions Catalyzed by a Chiral Bifunctional N-Heterocyclic Carbene with Noncovalent Activation. *Angew. Chem., Int. Ed.* **2022**, *61*, No. e202202040.
(77) Luo, Y.; Wei, Q.; Yang, L.; Zhou, Y.; Cao, W.; Su, Z.; Liu, X.; Feng, X. Enantioselective Radical Hydroacylation of α,β-Unsaturated Carbonyl Compounds with Aldehydes by Triplet Excited Anthraquinone. *ACS Catal.* **2022**, *12*, 12984−12992.
(78) Mo, Y.; Chen, Q.; Li, J.; Ye, D.; Zhou, Y.; Dong, S.; Liu, X.; Feng, X. Asymmetric Catalytic Conjugate Addition of Cyanide to Chromones and β-Substituted Cyclohexenones. *ACS Catal.* **2023**, *13*, 877−886.
(79) Pan, Z.-Z.; Pan, D.; Li, J.-H.; Xue, X.-S.; Yin, L. Copper(I)-Catalyzed Asymmetric Conjugate Addition of 1,4-Dienes to β-Substituted Alkenyl Azaarenes. *J. Am. Chem. Soc.* **2023**, *145*, 1749−1758.
(80) Xie, J.-H.; Hou, Y.-M.; Feng, Z.; You, S.-L. Stereodivergent Construction of 1,3-Chiral Centers via Tandem Asymmetric Conjugate Addition and Allylic Substitution Reaction. *Angew. Chem., Int. Ed.* **2023**, *62*, No. e2022163.

https://doi.org/10.1021/jacsau.3c00584
JACS Au 2024, 4, 164−176